RGNZ/MGPB

Geochemistry and petrography of metamorphic sole amphibolites from the Slatina Quarry, Mt. Zrinska Gora, Croatia

Rudarsko-geološko-naftni zbornik
(The Mining-Geology-Petroleum Engineering Bulletin)
UDC: 550.4; 552; 552.4
DOI: 10.17794/rgn.2024.2.8

Original scientific paper

Marija Putak Juriček[1]; Vesnica Garašić[2]

[1] *Department of Mineralogy, Georg-August-Universität Göttingen, Goldschmidtstr. 1, 37077 Göttingen, Germany, 0009-0008-7369-3676*
[2] *Faculty of Mining, Geology and Petroleum Engineering, University of Zagreb, Pierottijeva 6, 10 000 Zagreb, Croatia, 0002-4752-6937*

Abstract
The investigated Mt. Zrinska Gora amphibolites are a part of the metamorphic sole of the Banovina ophiolite complex. Mineral composition and other petrographic characteristics of amphibolites and adjacent peridotite were investigated by polarised microscopy and chemical analyses of rocks were obtained by a combination of inductively coupled plasma mass and emission spectrometry. The main minerals in these garnet-bearing amphibolites are amphibole and plagioclase with accessory garnet, sphene, spinel, opaque mineral ± clinopyroxene ± quartz ± actinolite ± zoisite-clinozoisite ± prehnite ± pumpelyite and ± clay minerals. Kelyphitic corona is developed around garnet. The amphibolites have nematoblastic, nematogranoblastic, porphyroblastic and porphyroclastic textures and homogenous to foliated structures. The presence of clinopyroxene in some of the investigated amphibolites points to their possible formation under P–T conditions of upper amphibolite facies. The greenschist facies retrograde metamorphism and subsequent surface weathering of amphibolites is also evident. The chemical composition of rocks indicates that protoliths of most amphibolites were tholeiitic basalts, initially formed in island arcs and the adjoining back-arc basins. During the intraoceanic subduction in Jurassic Neotethys Ocean basalts/basaltic tuffs of island arc tholeiite affinity and back-arc basin basalts, positioned on the top of the down-going oceanic slab, were welded to the base of the hot over-riding mantle wedge, metamorphosed to amphibolite rocks and obducted together with ophiolites on the Adria continental margine. The new described amphibolite type having peridotite protolith characteristics originated as the consequence of the hydration of the bottom part of the overlying mantle wedge.

Keywords:
amphibolite; metamorphic sole; peridotite; tholeiitic basalt; back-arc basin

1. Introduction

Amphibolite samples were collected from the Slatina Quarry in the vicinity of Gornji Klasnić, a small village located around 20 km south of Glina (see **Figure 1**). The investigated amphibolites are part of the metamorphic sole of the Banovina ophiolite complex (**Majer and Lugović, 1985**). Besides amphibolites, which constitute the upper part of the metamorphic sole, different metapelites (micaschists, gneisses, hornfelses, quartzites) occur in its lower part (**Majer and Lugović, 1985**). Banovina ophiolites occur within a NW–SE striking zone along the boundary between the Inner and Outer Dinarides. The Banovina ophiolite complex is thought to be the thrust over the Adriatic Carbonate Platform, which forms most of the Outer Dinarides. The Banovina ophiolite complex itself is a part of the Inner Dinarides and is comprised of typical oceanic crust and upper mantle lithologies (pelagic sediments, basalts, peridotites) along with various metamorphic members (amphibolites, amphibole schists, mica schists, gneisses, quartzites, hornfelses). The amphibolites are thought to have formed through metamorphism of the oceanic crust which existed between the Adriatic Carbonate Platform and the Eurasian Plate during the Jurassic (**Majer and Lugović, 1985**). This metamorphic event is presumably linked to the emplacement of the Banovina ophiolite complex. During the Upper Cretaceous and the Cenozoic, younger sediments were deposited over the ophiolite complex through multiple transgressive events (**Šikić et al., 1990; Šikić, 2014**). The dismembered ophiolite bodies are partially covered by younger sediments, which complicates the interpretation of geological relationships in the field.

The most detailed investigation of Banovina amphibolites was carried out by **Majer and Lugović (1985)**. They concluded, based on the petrographic and geochemical characteristics of the studied rocks, that amphibolites are orthometamorphites. The authors determined the tholeiitic affinity and within the plate signature of the amphibolite protoliths, including diabases and basalts, which originated by submarine eruptions.

Corresponding author: Vesnica Garašić
e-mail address: vesnica.garasic@rgn.unizg.hr

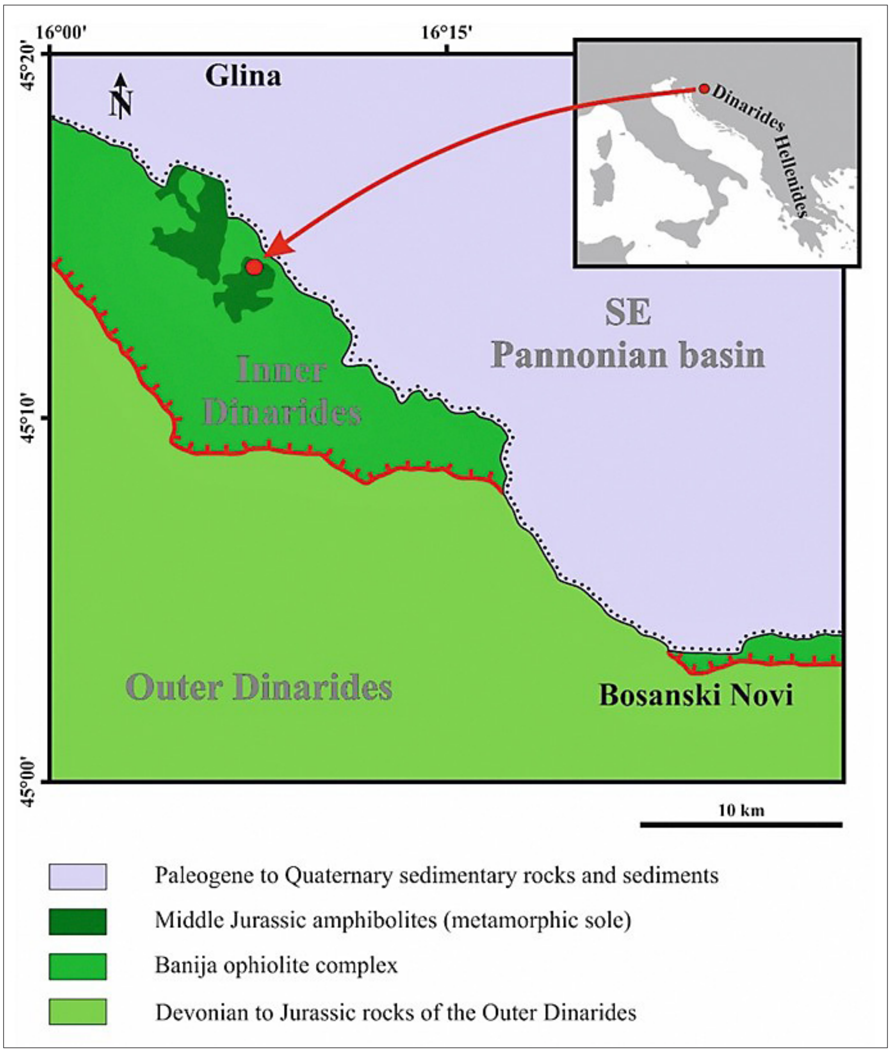

Figure 1: Schematic geological map of the investigated area after **Šikić et al. (1990)**.
Location of the Slatina Quarry from which the investigated amphibolites were taken is indicated in red.

The *K–Ar* radiometric dating of amphiboles from amphibolite yielded 166 ± 10 Ma for the metamorphic event. **Majer and Lugović (1985)** concluded that all metamorphic rocks in the Banovina ophiolite belt have been metamorphosed in the Middle Jurassic. Electron microprobe analyses of amphiboles characterised by low octahedral Al as well as generally low titanium content, along with anorthite content in plagioclase (>>An_{17}), suggest that metamorphism occurred at relatively low pressure and the temperature exceeding 520ºC (**Majer and Lugović, 1985**). The most recent field descriptions of amphibolite occurrences in Slatina Quarry are given in the PhD thesis written by **Bilić (2021)**.

Over the last several decades, new analytical methods were developed, and our understanding of ophiolite emplacement mechanisms evolved significantly (**Wakabayashi and Dilek, 2003, Kusky et al., 2013; Agard et al., 2018; Balen and Massonne, 2021**). As a result, a new investigation of Banovina amphibolites, solely the ones from the Slatina Quarry near Gornji Klasnić, was initiated. More detailed chemical analyses of amphibolites presented in this paper allowed a refinement of the original interpretation of the geotectonic setting of their protolith rocks done by **Majer and Lugović (1985)**. This study is a small contribution to the large body of previous work on ophiolites of the Mediterranean region (**e.g. Robertson, 2002; Dilek and Furnes, 2009; Schmid et al., 2008; Schmid et al., 2020; Šegvić et al., 2020; van Hinsbergen et al., 2020**) dedicated to the reconstruction of the sequence of tectonic events which led to the closure of the Tethys Ocean.

2. Methods

In the frame of the geological fieldwork, based on careful observation of different rock types and their mutual relationships, seven samples of amphibolites, two composite samples representing contact between amphibolite and peridotite and one sample of serpentinised peridotite were collected in the Slatina Quarry.

Copyright held(s) by author(s), publishing rights belongs to publisher, pp. 97-110, DOI: 10.17794/rgn.2024.2.8

The mineralogical-petrographic properties of all rock samples were determined using a polarisation microscope Leica Microsystem 020-522 101 DM/LSP with 4x, 10x and 40x magnifications and standard thin sections at the University of Zagreb, Faculty of Mining, Geology and Petroleum Engineering, Department of Mineralogy, Petrology and Mineral Resources. Microphotographs were taken applying a Leica DC100 camera and Leica IM50 software.

With relevance to their petrographic characteristics, amphibolite and peridotite from one composite sample and four other amphibolites were chosen for chemical analyses. For this purpose, the samples were broken into small pieces using a hand hammer and powdered in agate grinding vessels by its rotary motion in a Siebtechnik mill at the University of Zagreb Faculty of Mining, Geology and Petroleum Engineering, Department of Mineralogy, Petrology and Mineral Resources. The rock powders were air-dried and sent for chemical analyses to the Bureau Veritas Commodities Canada Ltd., in Vancouver. There, the rock powders were fused with pure lithium-tetraborate ($Li_2B_4O_7$) and lithium metaborate ($LiBO_2$) and then dissolved in a diluted nitric acid (HNO_3) solution. Major and trace element concentrations were determined using inductively coupled plasma emission spectroscopy (ICP-ES) and inductively coupled plasma mass spectrometry (ICP-MS), respectively. The internal geological reference material (STD SO-18) was used for the calibration.

3. Results

3.1. Field observation and sample collection

The investigated amphibolites form lenticular rock bodies (see **Figure 2**) surrounded by serpentinised peridotite (see **Figure 3**). Various types of amphibolites, characterised by different structural properties and colours, were observed. These range from darker and homogeneous to lighter-coloured and foliated types. It is noteworthy that different types of amphibolites may coexist within the same lenticular rock body (see **Figure 4**). Ten samples were collected in total (designated BN 14-1 to BN 14-10), including seven samples of different amphibolites, two composite samples from the peridotite-amphibolite contact and one sample of serpentinised peridotite. The sample BN 14-4, taken from the peridotite-amphibolite contact (see **Figure 3**), was separated into samples amphibolite BN 14-4A and peridotite BN 14-4B.

Figure 2: Outcrop of lenticular amphibolite rock bodies (A) surrounded by serpentinised peridotite

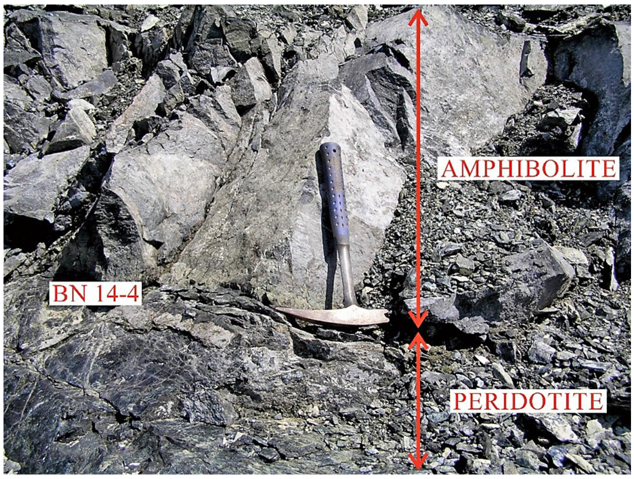

Figure 3: The sample BN 14-4 was collected at the contact between an amphibolite lens and surrounding peridotite

Figure 4: A fragment of an amphibolite lens containing both the foliated and homogeneous varieties of amphibolite

The six samples, investigated in detail by polarizing microscope, ICP-ES and ICP-MS are described here.

3.2. Petrographic characteristics of rocks

Sample BN 14-1 is a darker and structurally homogeneous variety of amphibolite. The rock is composed of hornblende (up to 80 vol. %), less abundant plagioclase (up to 15 vol. %) and a variety of accessory phases (1-5 vol. %) such as titanite, opaque minerals, garnet and quartz. The texture of the rock is nematogranoblastic

Copyright held(s) by author(s), publishing rights belongs to publisher, pp. 97-110, DOI: 10.17794/rgn.2024.2.8

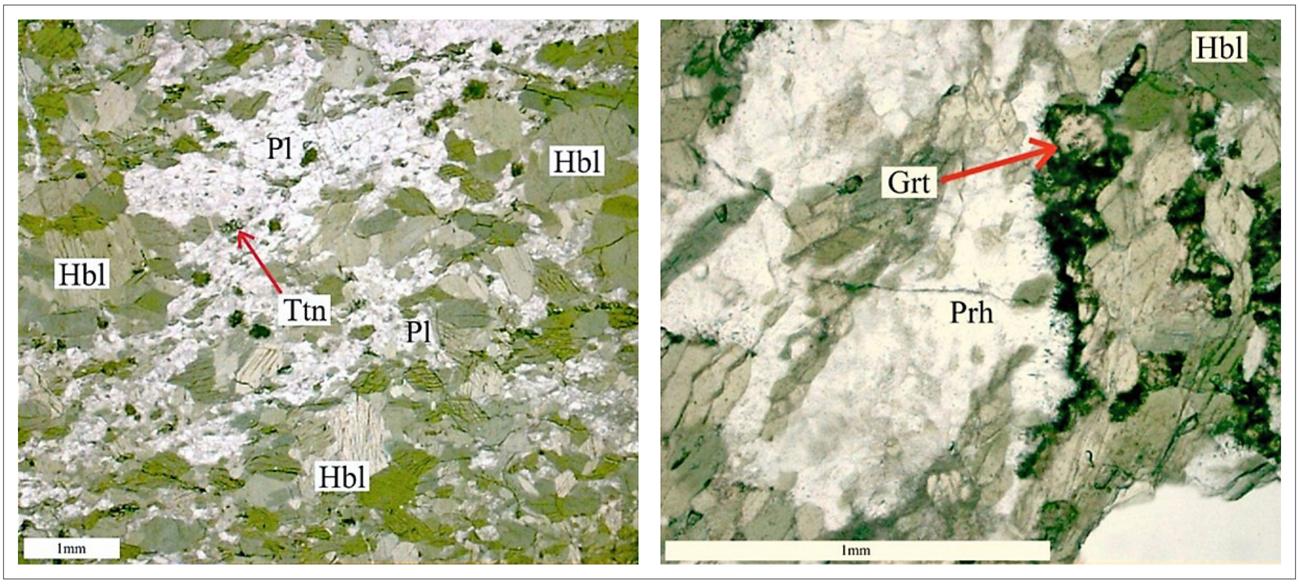

Figure 5: Left: Nematogranoblastic to porphyroblastic texture of BN 14-1 (N). Right: Garnet grain with a kelyphitic corona in BN 14-1 (N). Grt=garnet; Hbl=hornblende; Pl=plagioclase; Prh=prehnite; Ttn=titanite. Mineral abbrevations after Slovenec and Bermanec (2003).

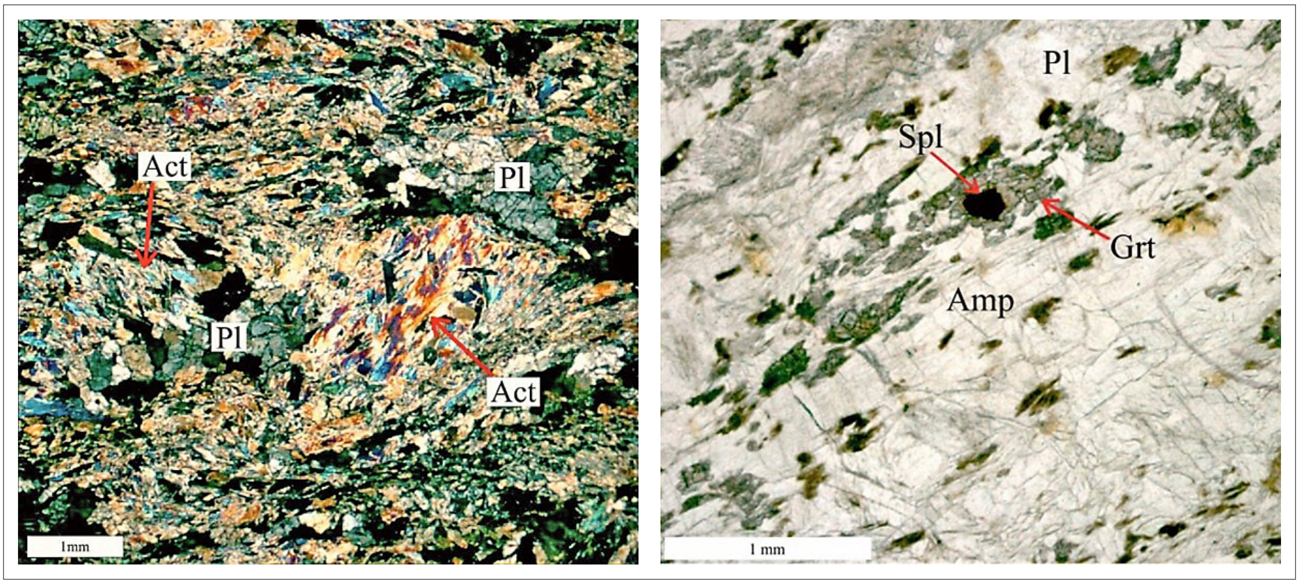

Figure 6: Left: Porphyroclastic texture of BN 14-6 (N+). Right: A spinel grain from BN 14-7 surrounded by garnet (N). Act=actinolite; Amp=amphibole; Grt=garnet; Pl=plagioclase; Spl=spinel. Mineral abbrevations after Slovenec and Bermanec (2003).

with sporadic porphyroblasts of hornblende (see **Figure 5**). Hornblende is unaltered and pleochroic ranging from light yellow green to darker green colour (X = light yellow green, Y = green, Z = light green). Most plagioclase grains are recrystallized as indicated by the relicts of larger and deformed plagioclase grains surrounded by smaller undeformed ones. Plagioclase is highly replaced by prehnite and, occasionally, by clay minerals as well. Garnet is often surrounded by kelyphitic corona (see **Figure 5**).

Samples BN 14-6, BN 14-7 and BN 14-10 represent the lighter and foliated variety of amphibolites. The sample BN 14-6 has nematogranoblastic to porphyroblastic texture. It contains hornblende (up to 70 vol. %) showing faint colourless to light green pleochroism (X = colourless to light yellow green, Y = light green, Z = light yellow green), which has been mostly altered to actinolite during retrograde metamorphism. Plagioclase (up to 30 vol. %), being almost completely transformed to zoisite-clinozoisite and clay minerals, occasionally forms eye-shaped (augen) mineral aggregates (see **Figure 6**). Sample BN-14-7 is characterized by a porphyroclastic texture and almost colourless to rarely pale green amphibole (up to 55 vol. %) which does not display pleochroism. The amphibole likely has a composition between tremolite and magnesiohornblende and is par-

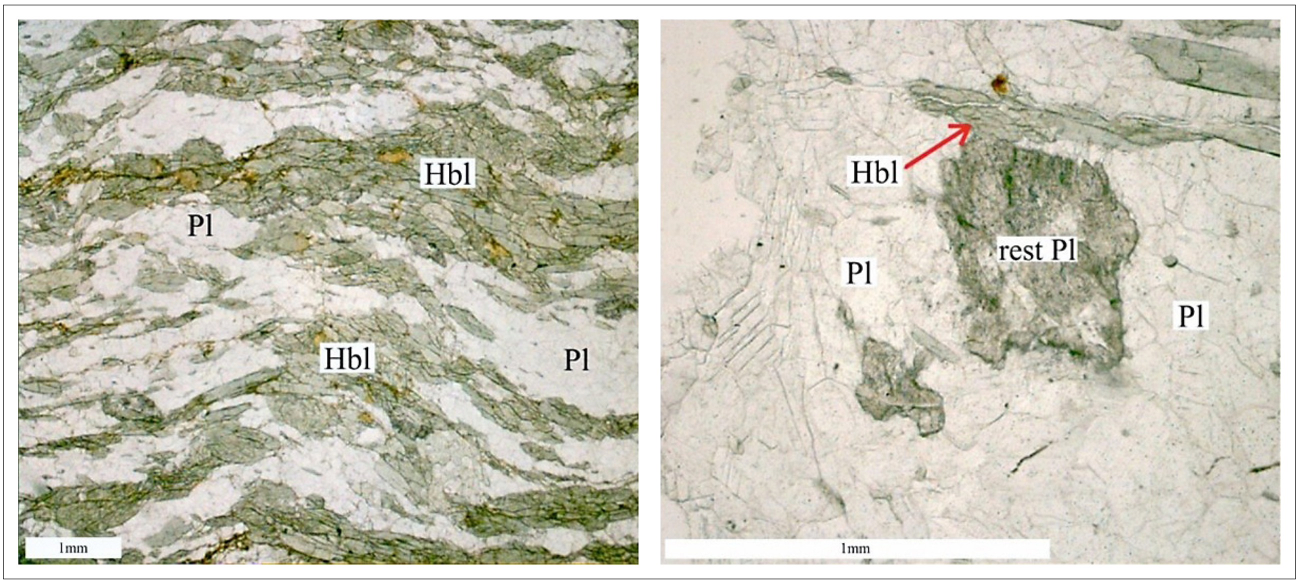

Figure 7: Left: Folding on the microscale in BN 14-10 (N). Right: Relict of the primary (magmatic) plagioclase altered to clay minerals and clinozoisite in BN 14-10 (N). Czo=clinozoisite; Hbl=hornblende; Pl=plagioclase; rest Pl=magmatic plagioclase relict. Mineral abbrevations after Slovenec and Bermanec (2003).

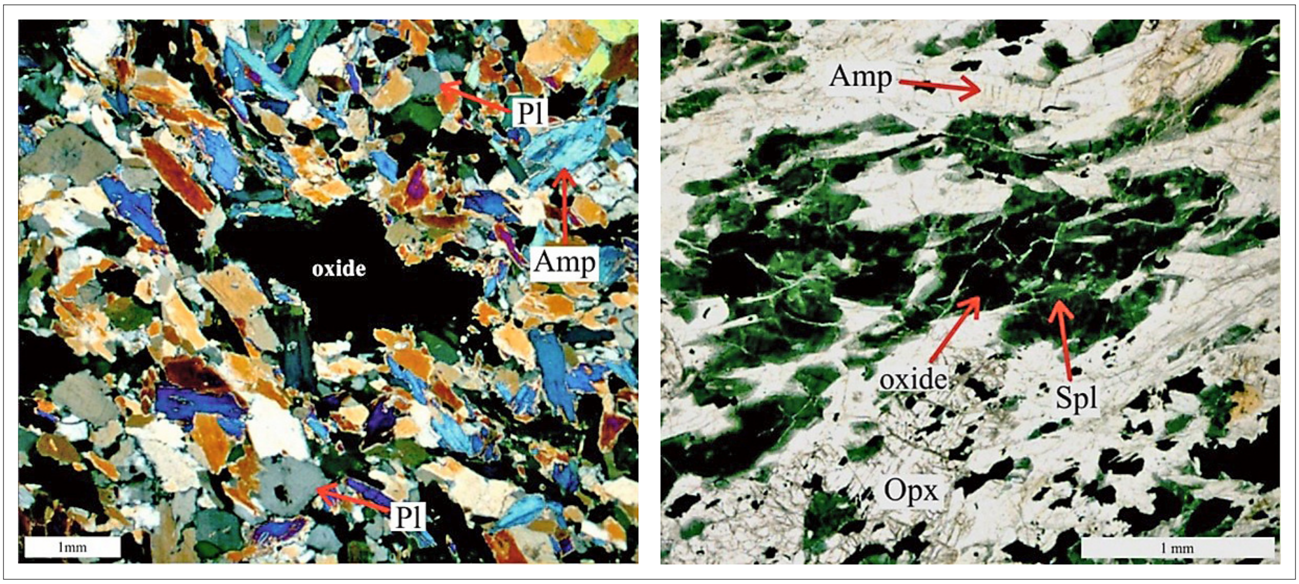

Figure 8: Left: Nematoglanoblastic texture of BN 14-4A (N+). Right: Green spinel surrounding opaque oxide mineral grains in BN 14-4B (N). Amp=amphibole; Opx=orthopyroxene; Pl=plagioclase; Spl=spinel. Mineral abbrevations after Slovenec and Bermanec (2003).

tially altered to actinolite. Plagioclase (up to 35 vol. %) display strong retrograde transformation to prehnite and in a lesser extent to clinozoisite. Another notable feature of BN 14-7 are brown spinel grains surrounded by garnet with kelyphitic coronas. Spinel and garnet, occurring in this sample in a significantly greater amount (up to 10 vol. %) than in other amphibolites, form thin parallel laminae and lenses, giving the rock a distinct foliated structure (see **Figure 6**). Nematoblastic to porphyroblastic sample BN-14-10 contains unaltered hornblende (up to 65 vol. %) with light to darker green pleochroism (X = light yellow green, Y = green, Z = light green). Recrystallized plagioclase grains are unaltered as well. Several large mineral aggregates of clinozoisite, prehnite, pumpellyite and clay minerals (see **Figure 7**) were observed in this sample. They were interpreted as relict plagioclase grains. The rock also contains accessory titanite.

Sample BN 14-4A is an amphibolite taken from the amphibolite-peridotite contact. The rock has a nematogranoblastic texture (see **Figure 8**) and it differs mineralogically from the other amphibolites. The sample is unaltered and contains a Mg-rich amphibole (up to 85 vol. %) which does not display pleochroism. Mg-rich amphibole has high second-order interference colours and extinction angles between 10° and 18°. Occasional-

Table 1: Major element concentrations (wt.%)

Rock	amphibolite	amphibolite	peridotite	amphibolite	amphibolite	amphibolite
Remark	homogeneous	contact	contact	foliated	foliated	foliated
Sample	**BN 14-1**	**BN 14-4A**	**BN 14-4B**	**BN 14-6**	**BN 14-7**	**BN 14-10**
SiO_2	45.28	39.95	32.36	44.83	39.34	49.11
TiO_2	1.03	0.19	0.37	0.12	0.04	0.23
Al_2O_3	14.93	12.00	16.75	18.33	23.11	15.37
Fe_2O_3	9.12	12.30	19.84	3.56	3.37	6.17
Cr_2O_3	0.080	0.142	0.111	0.159	0.402	0.128
MnO	0.14	0.09	0.11	0.07	0.05	0.11
MgO	10.88	21.96	20.32	12.19	11.90	12.00
CaO	14.51	5.62	3.38	16.94	15.46	13.97
Na_2O	1.20	0.11	0.12	0.50	0.40	1.01
K_2O	0.18	<0.01	<0.01	0.02	0.06	0.05
P_2O_5	0.07	<0.01	<0.01	<0.01	<0.01	<0.01
LOI	2.3	7.2	6.2	3.1	5.6	1.6
Σ	99.73	99.61	99.62	99.78	99.79	99.76

ly, amphibole grows around clinopyroxene grains which are thought to be a restite of the primary assemblage. Plagioclase (up to 12 vol. %) is present in a considerably lesser extent in comparison with other amphibolites. Sample BN 14-4A also contains accessory minerals (up to 3 vol. %) quartz, garnet and coarse opaque mineral, presumably spinel.

Sample 14-4B is a porphyroclastic spinel harzburgite. The primary mineral paragenesis consists of olivine, orthopyroxene and an opaque oxide phase, most likely spinel. Opaque spinel is surrounded by a green mineral (see **Figure 8**). Most olivine grains are serpentinised and some orthopyroxene grains have been transformed into a Mg-rich amphibole like the one present in BN 14-4A. Small quantities of retrograde actinolite can be found in BN 14-4B as well.

3.3. Chemical composition

With relevance to their petrographic characteristics, amphibolite and peridotite from one composite sample and four other amphibolites were chosen for chemical analyses.

3.3.1. Major elements

Major element concentrations of the analysed samples, expressed in wt. %, are shown in **Table 1**.

The SiO_2 content in the analysed amphibolites ranges from 39.34 to 49.11 wt.%, whereas their Al_2O_3 content varies between 12.00 and 23.11 wt.% with BN 14-7 being considerably more aluminous than the other samples. The high aluminium content of BN 14-7 is due to the presence of significant modal proportions of spinel and garnet in the sample. Amphibolites contain 3.37 to 12.30 wt.% and 10.88 to 21.96 wt.% of Fe_2O_3 and MgO, respectively. The CaO content of amphibolites ranges from 5.62 to 16.94 wt.%. While the samples have variable major element composition, it can be observed that BN 14-4A, sampled from the contact with peridotite BN 14-4B, is significantly more Mg-rich and Ca-depleted (see **Table 1**) than the remaining amphibolites. Overall Na_2O and K_2O contents of analysed rocks are quite low, although BN 14-1 is slightly more alkali enriched in comparison to other amphibolites. BN 14-1 is also more Ti-rich than other samples due to the higher amount of modal titanite observed in this sample. Losses on ignition (LOI) in amphibolite analyses vary between 1.6 and 7.2 wt.%. As amphibole itself contains approximately 2 wt.% of water, amphibolite samples with LOI < 2 wt.% may be considered unaltered, while greater LOI should be attributed to the presence of secondary hydrous minerals in the rock (e.g. prehnite). Major element compositions of the two foliated amphibolites BN 14-6 and BN 14-10 are relatively similar, while the third foliated sample BN 14-7 contains considerably less silica and more aluminium. This difference in major element composition of BN 14-7 in comparison to the other two foliated amphibolites may be due to either higher degree of alteration (LOI 5.6 wt.%) or a difference in the composition of the protolith. Notably, peridotite sample BN 14-4B has a quite similar major element composition to amphibolite BN 14-4A.

3.3.2. Trace elements

Trace element concentrations of all six samples, expressed in ppm, are listed in **Table 2** and depicted graph-

Copyright held(s) by author(s), publishing rights belongs to publisher, pp. 97-110, DOI: 10.17794/rgn.2024.2.8

Table 2: Trace element concentrations (ppm).

Rock	amphibolite	amphibolite	peridotite	amphibolite	amphibolite	amphibolite
Remark	homogeneous	contact	contact	foliated	foliated	foliated
Sample	**BN 14-1**	**BN 14-4A**	**BN 14-4B**	**BN 14-6**	**BN 14-7**	**BN 14-10**
Ag	<0.1	<0.1	<0.1	<0.1	<0.1	<0.1
As	<0.5	0.5	<0.5	1.2	12.1	<0.5
Au	2.6	<0.5	1.0	<0.5	<0.5	<0.5
Ba	45	1	2	4	20	10
Be	1	<1	2	<1	<1	<1
Bi	<0.1	<0.1	<0.1	<0.1	<0.1	<0.1
Cd	<0.1	<0.1	<0.1	<0.1	<0.1	<0.1
Co	43.7	115.2	145.1	31.0	33.0	39.6
Cs	<0.1	0.2	<0.1	<0.1	<0.1	<0.1
Cu	75.3	10.3	12.9	21.4	1.0	6.3
Ga	13.3	9.2	13.5	8.9	8.4	9.1
Hf	1.8	0.2	0.6	0.1	<0.1	0.2
Hg	<0.01	<0.01	<0.01	<0.01	<0.01	<0.01
Mo	<0.1	<0.1	<0.1	<0.1	<0.1	<0.1
Nb	5.1	0.4	0.5	0.2	<0.1	0.2
Ni	33.3	404.1	414.0	70.9	217.7	11.6
Pb	0.5	0.3	0.1	0.1	0.3	0.5
Rb	1.8	0.2	0.2	0.2	1.4	0.8
Sb	<0.1	<0.1	<0.1	<0.1	<0.1	<0.1
Sc	32	21	33	25	2	36
Se	<0.5	<0.5	<0.5	<0.5	<0.5	<0.5
Sn	<1	<1	<1	<1	<1	<1
Sr	198.7	5.6	6.8	77.0	102.8	130.6
Ta	0.4	<0.1	<0.1	<0.1	<0.1	<0.1
Th	0.5	<0.2	<0.2	<0.2	<0.2	<0.2
Tl	<0.1	<0.1	<0.1	<0.1	<0.1	<0.1
U	0.1	<0.1	0.1	<0.1	<0.1	<0.1
V	222	104	197	95	25	142
W	<0.5	<0.5	0.5	0.9	<0.5	<0.5
Y	20.7	3.1	6.3	2.7	0.5	4.6
Zn	4	15	15	5	2	2
Zr	62.6	6.6	19.9	3.1	1.3	5.0
La	5.4	0.8	1.3	0.2	0.2	0.6
Ce	12.4	1.4	2.6	0.6	0.3	1.7
Pr	1.67	0.11	0.35	0.07	<0.02	0.20
Nd	8.1	0.6	1.6	0.5	<0.3	1.2
Sm	2.65	0.28	0.78	0.24	0.07	0.60
Eu	0.88	0.07	0.12	0.16	0.09	0.34
Gd	3.24	0.47	1.02	0.35	0.08	0.80
Tb	0.61	0.10	0.19	0.07	0.02	0.15
Dy	3.90	0.67	1.21	0.51	0.15	0.91
Ho	0.77	0.12	0.24	0.11	<0.02	0.19
Er	2.15	0.37	0.74	0.32	0.07	0.55
Tm	0.32	0.05	0.11	0.04	<0.01	0.08
Yb	2.18	0.38	0.84	0.31	0.06	0.50
Lu	0.33	0.07	0.14	0.05	<0.01	0.08
Eu/Eu*	0.92	0.59	0.41	1.69	3.68	1.5

$Eu/Eu^* = Eu_N / ((Sm_N) \times (Gd_N))^{1/2}$ (after **Rollinson, 1993**)

Copyright held(s) by author(s), publishing rights belongs to publisher, pp. 97-110, DOI: 10.17794/rgn.2024.2.8

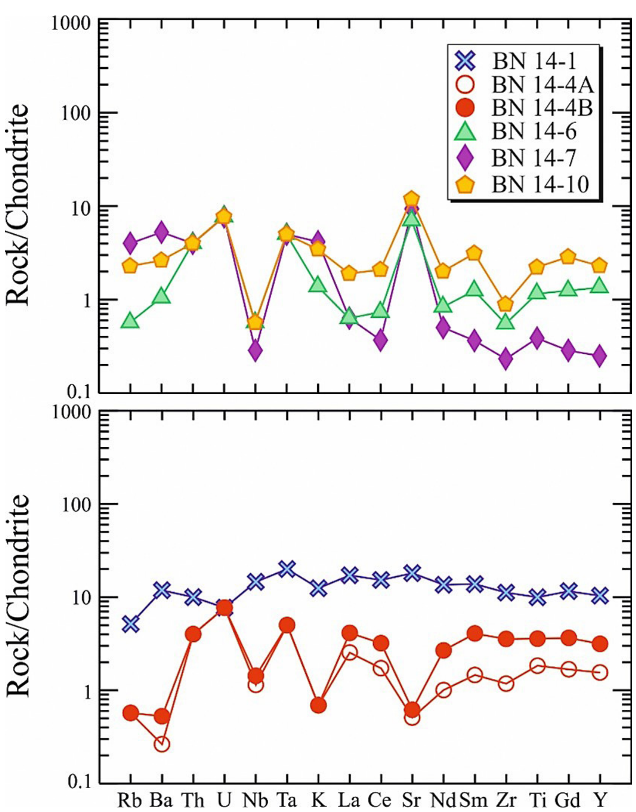

Figure 9: Chondrite normalised spider diagrams. Normalisation values are after Sun and McDonough (1989). Trace element distribution of peridotite sample BN-14B is indicated by full red circles and all other symbols represent different amphibolite samples.

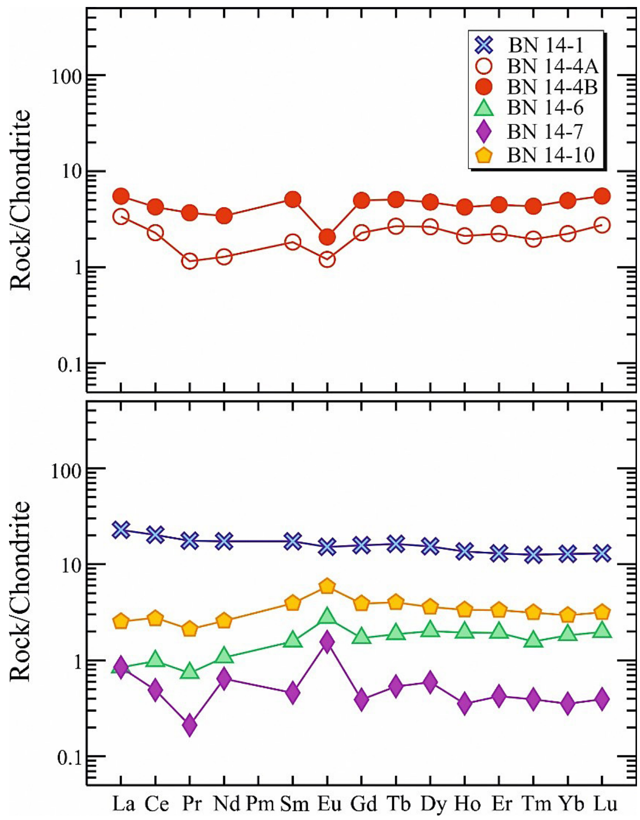

Figure 10: Chondrite normalised REE diagrams. Normalisation values are after Sun and McDonough (1989). Trace element distribution of peridotite sample BN-14B is indicated by full red circles and all other symbols represent different amphibolite samples.

ically in chondrite-normalized spider diagrams (see **Figure 9**) and REE diagrams (see **Figure 10**), both according to **Sun and McDonough (1989)**. Three different trace element distribution patterns may be observed (see **Figures 9** and **10**).

Samples BN 14-4A (amphibolite) and BN 14-4B (peridotite), taken from the contact of an amphibolite lens with the surrounding serpentinised peridotite, display a mutually similar trace element distribution pattern. In comparison to chondrite values, these samples are depleted in Rb, Ba, K and Sr and enriched in U, Th, Ta, La, Ce, Zr, Ti and HREEs. The samples show negative Nb and Sr anomaly coupled with a positive Ta anomaly in a spider diagram (see **Figure 9**). A negative Eu anomaly is observed in the REE diagram (see **Figure 10**) with Eu/Eu* ratios of 0.59 in sample BN 14-4A and 0.41 in BN 14-4B, according to equation of **Rollinson (1993)**: $Eu/Eu^* = Eu_N /((Sm_N) \times (Gd_N))^{1/2}$. The REE in both samples are enriched 1 to 6 times in relation to chondrite.

While sample BN 14-7 has a somewhat different major element composition than samples BN 14-6 and BN 14-10, they all display similar trace element distribution patterns in spider and REE diagrams (see **Figure 9** and **10**) and share some petrographic characteristics (lighter colour and foliated structure). Amphibolites BN 14-6, BN 14-7 and BN 14-10 show negative Nb and mildly pronounced negative Zr anomaly, but positive Sr anomaly in a spider diagram (see **Figure 9**). They also display a positive Eu anomaly (Eu/Eu* values 1.50-3.69) in the REE diagram (see **Figure 10**).

The darker and homogeneous variety of amphibolites, represented by sample BN 14-1, has a significantly different geochemical fingerprint compared to the other samples. Sample BN 14-1 shows a relatively flat pattern in the spider diagram (see **Figure 9**) with element concentrations being 5 to 20 times enriched relative to chondrite. In the REE diagram this sample demonstrate slightly LREE-enriched pattern, where element concentrations are 15 to 25 times higher in comparison to chondrite (see **Figure 10**).

4. Discussion

4.1. Field relationships and petrographic characteristics

The investigated amphibolites comprise a part of the metamorphic sole of the Banovina ophiolite complex (**Majer and Lugović, 1985**). They form lenticular rock bodies surrounded by serpentinised peridotite, a field relationship presumably attained during the ocean-ocean

Copyright held(s) by author(s), publishing rights belongs to publisher, pp. 97-110, DOI: 10.17794/rgn.2024.2.8

subduction and subsequent emplacement of the ophiolite on the continental margin. The amphibolites are petrographically heterogeneous with nematoblastic, nematogranoblastic and porphyroblastic textures and have homogeneous to foliated structures. Porphyroclastic texture observed in one amphibolite sample is likely a result of post-metamorphic brittle deformation of rocks. Evidence of greenschist facies retrograde metamorphism and surface weathering of amphibolites was observed and the foliated variety appears to be more susceptible to alteration. Some of amphibolites contain relict clinopyroxene and plagioclase grains, both of which most likely represent the remnants of the primary paragenesis of the protolith. Although such amphibolites are not typical pyroxene amphibolites, they could point to the lower border of upper amphibolite facies (**Majer and Lugović, 1985**).

4.2. Para-versus orthoamphibolites

Previous investigations have shown that Banovina amphibolites are orthometamorphic (**Majer and Lugović, 1985**) and the low SiO_2 contents (Table 1: SiO_2 = 39.34-49.11 wt.%) of the investigated rocks suggest basic to ultrabasic character of the protolith. A sedimentary protolith would be expected to have significantly higher alkali and SiO_2 contents. High concentrations of some major element oxides (Table 1: MgO = 10.88-21,96 wt.%; Cr_2O_3 = 0.080-0.402 wt.%) and of certain trace elements (Table 2: Ni = 11.6-404.1 ppm; Co = 31.0-115.2 ppm) are also consistent with the conclusion that amphibolite protolith rocks were of basic to ultrabasic character. Furthermore, **Majer and Lugović (1985)**, who studied a greater number of samples collected from a larger area, have described relict magmatic textures in several amphibolite samples.

4.3. Chemical classification and determination of magmatic series of protolith(s)

Although not shown here, a TAS diagram after **Le Maitre (1989)** was applied for the protolith classification of orthoamphibolites. Samples BN 14-1, BN 14-6 and BN 14-10 plot in the basalt field while more Mg-rich samples BN 14-4A and BN 14-7 plot into the field of picrobasalt. Since alkalis and large ion lithophile elements may be mobile during metamorphism, trace elements and their ratios have been used for a better classification. The peridotite sample BN 14-4B was omitted in Figures 11 to 14, since these diagrams are intended exclusively for the classification of basic rocks. In the Zr/Ti-Nb/Y diagram after **Pearce (1996)** all samples plot in the field of subalkaline basalts (see **Figure 11**).

In the TiO_2-Zr/(P_2O_5*10^4) diagram (**Winchester and Floyd, 1977**) and the Nb/Y-Zr/(P_2O_5*10^4) diagram (**Floyd and Winchester, 1975**), which is not shown here, all of the samples plot in the field of tholeiitic (subalkaline) basalts (see **Figure 12**).

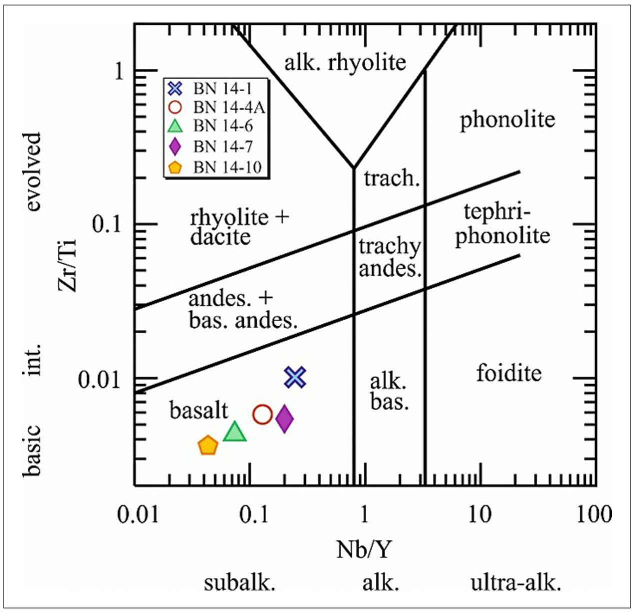

Figure 11: Zr/Ti-Nb/Y classification diagram after Pearce (1996)

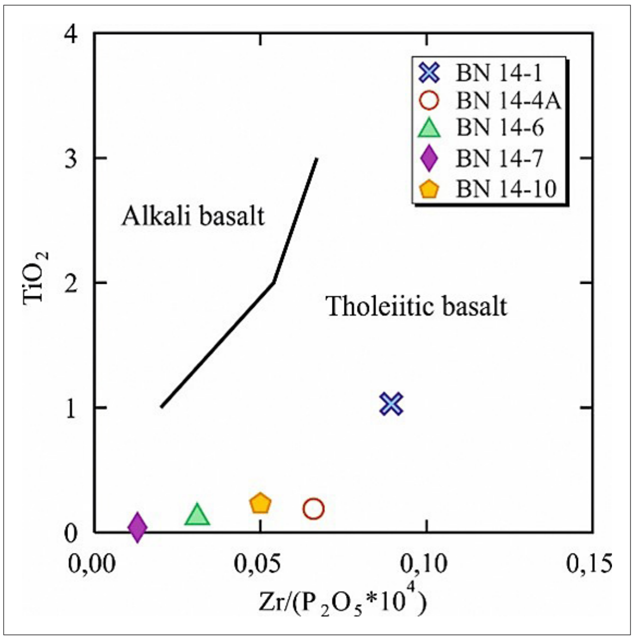

Figure 12: TiO_2-Zr/(P_2O_5*10^4) diagram after Winchester & Floyd (1977)

Based on the chemical analyses of a larger number of samples and using both an AFM diagram (**Irvine and Baragar, 1971**) and diagrams after **Miyashiro (1975)**, **Majer and Lugović (1985)** have also concluded that amphibolites had protoliths of tholeiitic character.

4.4. Geotectonic setting of the protolith(s)

The investigated amphibolites displaying not only three distinctive trace element patterns (see **Figures 9** and **10**), but also different major element compositions (see **Table 1**) and structures (see **Figure 4**), are indicative of protoliths originated in disparate geotectonic settings.

Copyright held(s) by author(s), publishing rights belongs to publisher, pp. 97-110, DOI: 10.17794/rgn.2024.2.8

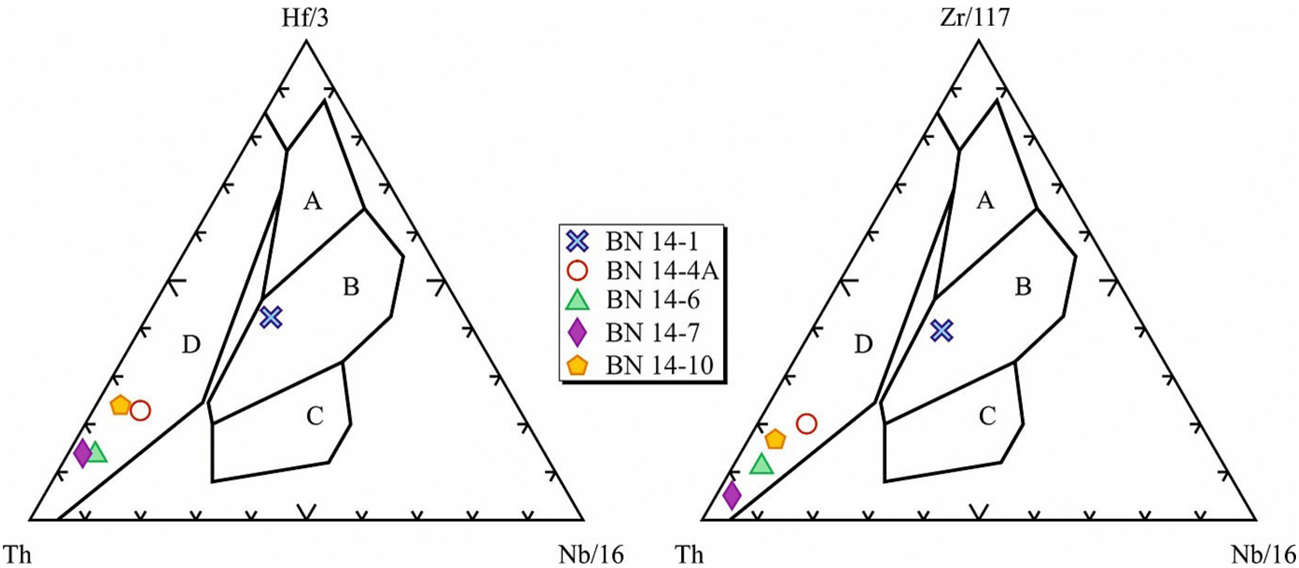

Figure 13: Th-Hf/3-Nb/16 and Th-Zr/117-Nb/16 diagrams after Wood (1980). A=N-MORB (Normal Mid-Ocean Ridge Basalt); B=E-MORB (Enriched Mid-Ocean Ridge Basalt); C=OIB (Ocean Island Basalt); D=IAT (Island Arc Tholeiite).

A representative of the darker coloured homogeneous variety of amphibolite, sample BN 14-1, plots into the field of enriched mid-ocean ridge basalts (E-MORB) (see **Figure 13**) in Th-Hf/3-Nb/16 and Th-Zr/117-Nb/16 diagrams after **Wood (1980)**, while it displays mid-ocean ridge basalt/back-arc basin basalt (MORB/BABB) geochemical characteristics (see **Figure 14**) according to V-Ti/1000 diagram after **Shervais (1982)**. In the new discrimination diagram after **Saccani (2015)** sample BN 14-1 plotted into the BABB field (see **Figure 14**), indicative of mature intra-oceanic back-arcs (showing no input of subduction or crustal components). In the chondrite normalised REE and spider diagrams (see **Figures 9** and **10**), sample BN 14-1 exhibits E-MORB like trace element patterns. Back-arc basins are extensional environments, resembling mid-ocean ridges. BAB basalts may have a geochemical fingerprint very similar to MORBs but may also display subduction-like trace element patterns due to the influence of subduction-zone fluids (**Wilson, 1989**). If the protolith of sample BN 14-1 had a back-arc basin origin, this could overall account for its trace element composition.

Foliated amphibolite samples BN 14-6, BN 14-7 and BN 14-10 plot into the island arc tholeiite (IAT) field (see **Figure 13**) in Th-Hf/3-Nb/16 and Th-Zr/117-Nb/16 diagrams after **Wood (1980)**. In the V-Ti/1000 diagram after **Shervais (1982)**, these samples plot between the low-Ti IAT/boninitic and IAT field (see **Figure 14**). Consistently, according to Th_N-Nb_N diagram after **Saccani (2015)**, samples BN 14-6, BN 14-7 and BN 14-10 have geochemical characteristics of intra-oceanic arcs (see **Figure 14**). In chondrite-normalised spider diagrams, foliated amphibolites display a sawtooth trace element pattern enriched in fluid-mobile incompatible elements (Rb, Ba, U, Sr) and depleted in HFSE elements (Nb, Ti, Zr, HREEs) which is typically associated with subduction zones (see **Figure 9**). The tholeiitic character of the samples is consistent with the island arc, rather than continental arc, setting of the protolith.

The sample BN 14-4A and foliated amphibolite samples plot together in discrimination diagrams, showing an IAT geochemical affinity. However, field relationships (BN 14-4A was taken from the amphibolite-peridotite contact) and chemical analyses suggest that this sample originates from an ultramafic protolith. Amphibolite sample BN 14-4A has a trace element distribution similar to the adjoining peridotite sample BN 14-4B (see **Figures 9** and **10**). Major element composition (low SiO_2 and CaO content, high MgO content, see **Table 1**) and the presence of high-Mg amphibole, an assumption based on the absence of pleochroism in the amphibole, in both BN 14-4A and BN 14-4B further support this conclusion.

Majer and Lugović (1985) had previously determined the orthomagmatic character of the Banovina amphibolites and presumed their tholeiitic affiliation. These opinions are supported by the data presented in this paper. Nevertheless, considering both a wide array of trace element concentrations and using discrimination diagrams which were unavailable at the time of the previous study, a more detailed interpretation of amphibolite protolith(s) initial geotectonic setting was obtained.

The appearance of different petrographic varieties of amphibolites and the overall geochemical data suggest at least three different protoliths: basalts of both IAT and BAB affinity, as well as ultramafic rocks. This is consistent with the interpretation that the investigated amphibolites are a part of the metamorphic sole of Banovina ophiolite complex and suggests that most of the amphibolite protoliths formed in intra-oceanic arc and back-arc basin environments, instead of a submarine within-plate setting as previously thought (**Majer and Lugović, 1985**).

Copyright held(s) by author(s), publishing rights belongs to publisher, pp. 97-110, DOI: 10.17794/rgn.2024.2.8

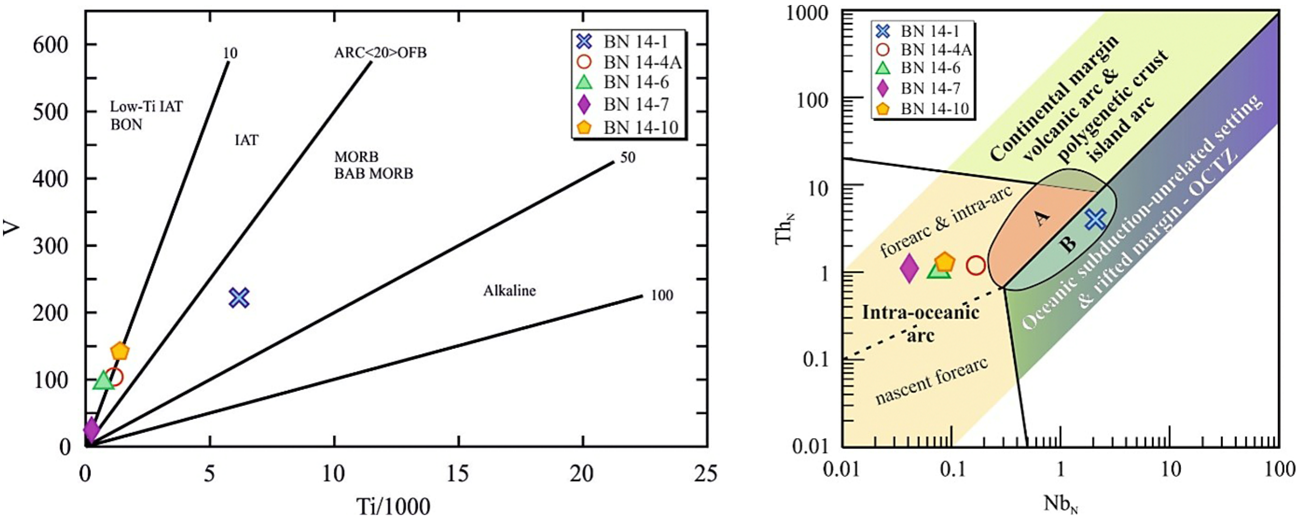

Figure 14: Left: V-Ti/1000 diagram after Shervais (1982). Right: Th_N-Nb_N diagram after Saccani (2015). A= immature back-arc basin basalts with an input from subduction or crustal components; B= mature back-arc basin basalts with no input from subduction or crustal components.

4.5. Origin of the metamorphic sole amphibolite in Banovina ophiolite complex (Slatina Quarry)

It is generally accepted that metamorphic soles form at the beginning of intraoceanic subduction, representing small pieces of a down-going oceanic slab, which are afterwards detached from the upper part of the subducting slab, accreted below the hot upper plate mantle wedge, metamorphosed and obducted together with ophiolites on the continental margin (**Daşçi et al., 2014; Soret et al., 2019**).

Basalts of both IAT and BAB affinity, found to be protoliths of amphibolites investigated in this study, suggest that intraoceanic subduction in Jurassic Neotethys Ocean, being in this area the result of convergence between Adria and Europe continental plates, started in the vicinity of the island arc and back arc basin. The fact that these two different types of amphibolite protoliths may coexist within the same lenticular rock body (see **Figure 4**) allows us to assume that back arc basin basalts were covered by basaltic tuff of IAT affinity, originated from neighbouring volcanic arc. During the intraoceanic subduction BAB basalts and basalts/basaltic tuffs of IAT affinity, positioned on the top of the down-going oceanic slab, were welded to the base of the hot over-riding mantle wedge, metamorphosed and obducted together with ophiolites on the Adria continental margin. The occurrence of ultramafic protolith of investigated amphibolites points to the hydration of the bottom part of the overlying mantle wedge (**Wada et al., 2012**) and its metamorphism during this intraoceanic subduction. Such an amphibolite (sample BN-14-4A) remained spatially associated with its protolith (sample BN-14-4B), as shown in **Figure 3**, and was exhumated and obducted on the Adria continental margin.

4.6. Comparison of studied amphibolites with contemporaneous Krivaja-Konjuh metamorphic sole amphibolites

Banovina ophiolite complex belongs to the Jurassic Central Dinaridic Ophiolite Belt (CDOB) which represents a part of the Tethyan ophiolite belt, extending from the European Alps to the southern Tibet. Many of the Tethyan ophiolite complexes are underlain by a sole of metamorphic rocks (**Dilek and Furnes, 2019**). The existence of island arcs with developed back-arc basins in the Tethyan region during the Jurassic is also supported by the results of many other studies on SE European ophiolites (**e.g. Dilek and Furnes, 2009; Daşçi et al., 2014; Šegvić et al., 2019**).

Comparison of the amphibolites studied here with well investigated metamorphic sole amphibolites of Krivaja-Konjuh ophiolite complex (**Šegvić et al., 2019; Šegvić et al., 2020; Balen and Massonne, 2021**) revealed remarkable similarities between them. Krivaja-Konjuh ophiolite complex is situated ~ 280 km to the east of Banovina ophiolite complex in central Bosnia and Herzegovina and represents the biggest ultramafic exposure in the Dinarides (**Šegvić et al., 2019**). Its metamorphic sole consists of metabasaltic and metapelitic rocks belonging to varieties from greenschist to granulite facies (**Šegvić et al., 2020**). *Sm-Nd* geochronology on granulite facies amphibolite gave the age of 162± 14 Ma, representing peak metamorphism rather than post-peak exhumation or the obduction process (**Šegvić et al., 2020**). The *K–Ar* radiometric dating of amphiboles from metamorphic sole amphibolite of Banovina ophiolite complex yielded 166 ± 10 Ma for the metamorphic event (**Majer and Lugović, 1985**). Peak temperature and pressure conditions for metamorphic sole amphibolites of Krivaja-Konjuh ophiolite complex, calculated from different mineral pairs, using an electron microprobe, were determinated to be in the range between 850 and 1100ºC at 1.1 to 1.3 GPa (**Šegvić et al., 2019**). **Balen and Massonne (2021)** using pressure-temperature (P-T) pseudosections, constructed in the MnNCKFMASHTO system with isopleths for the modal and chemical composition of minerals, obtained maximum P-T conditions at ca 2.1 GPa and 810ºC for garnet amphibolite (a clockwise P-T path) and maximum P-T conditions at 1.2 GPa and 960ºC for pargasite amphibolite (a counterclockwise P-T path). Interestingly, these estimates are reasonably similar to the new numerical simulations of slab temperature evolution during subduction initiation (**Holt and Condit, 2021**). For young (< 5Ma) subduction zones, the models generally yield temperatures between 800 and 1000°C at depths corresponding to pressures of 1 to 2 GPa.

The geochemistry of amphibolites from the metamorphic sole of the Krivaja-Konjuh ophiolite complex revealed that protoliths were magmatic rocks formed in the back-arc setting, principally as IAT-type gabbroic rock or MORB-like type extrusives (**Šegvić et al., 2019**) and mantle peridotite (**Balen and Massonne, 2021**). This is in accordance with protolith types estimated for the metamorphic sole amphibolites of Banovina ophiolite complex in this study. More detailed studies of metamorphic sole amphibolites of the Banovina ophiolite complex, including electron microprobe data and more precise geochronological data are necessary for a better understanding and reconstruction of the events which led to the closure of this part of the Tethys Ocean.

5. Conclusion

The main findings of this study are:

1. Genetic and spatial relationships between the studied amphibolites and the surrounding peridotites in the Slatina Quarry are consistent with the opinion of **Majer and Lugović (1985)** that these amphibolites have been formed as a part of the metamorphic sole of the Banovina ophiolite complex.
2. The new geochemical analyses of the studied amphibolites confirmed the findings of **Majer and Lugović (1985)**, who found that the protoliths of amphibolites are magmatic rocks and have tholeiitic character.
3. A new type of amphibolite is described in the Slatina Quarry, whose protolith, according to the geochemical data, was a peridotite.
4. Geochemical data suggest that most of the amphibolite protoliths have been formed in island arc and back-arc basin environments, instead of a submarine within-plate geotectonic setting as previously thought by **Majer and Lugović (1985**).
5. A model of amphibolite formation in the Banovina ophiolite complex is proposed, which includes an intraoceanic subduction in the Jurassic Neotethys Ocean, in the vicinity of island arc and back arc basin. During the intraoceanic subduction BAB basalts and basalts/basaltic tuffs of IAT affinity, positioned on the top of the down-going oceanic slab, were welded to the base of the hot over-riding mantle wedge, metamorphosed and obducted together with ophiolites on the Adria continental margin. The newly described amphibolite type has peridotite protolith characteristics formed as the consequence of the hydration of the bottom part of the overlying mantle wedge.

Acknowledgement

This work was supported financially by Ministry of Science and Education, Republic of Croatia in the scope of the scientific project: „Magmatism and mineral deposits of Dinaride carst area, No. 195-1953068-3206. We thank **Dražen Balen** and two other anonymous reviewers for their helpful comments and constructive criticism which significantly improved the quality of this paper.

6. References

Agard, P., Plunder, A., Angiboust, S., Bonnet, G. and Ruh, J. (2018): The subduction plate interface: rock record and mechanical coupling (from long to short timescales). Lithos, 320–321, 537–566. https://doi.org/10.1016/j.lithos.2018.09.029

Balen, D. and Massonne, H.-J. (2021): Two contrasting P-T paths for metamorphic sole amphibolites of the Dinaride Ophiolite Zone (Krivaja-Konjuh ultramafic massif, Central Bosnia and Herzegovina) and their geodynamic implicatons. Lithos, 394-395, https://doi.org/10.1016/j.lithos.2021.106184.

Bilić, Š. (2021): Petrogeneza peridotita i piroksenita na području Banovine, Hrvatska (*Petrogenesis of peridotites and pyroxenites in the area of Banovina, Croatia*). Unpublished Doctoral thesis, 226 p. (*in Croatian – with English abstract).*

Daşçi, H.T., Parlak, O., Nurlu, N. and Billor, Z. (2014): Geochemical characteristics and age of metamorphic sole rocks within a Neotethyan ophiolitic mélange from Konya region (central southern Turkey). Geodinamica Acta. https://doi.org/10.1080/09853111.2014.979532

Dilek, Y. and Furnes, H. (2009): Structure and geochemistry of Tethyan ophiolites and their petrogenesis in subduction rollback systems. Lithos, 113, 1-20. https://doi.org/10.1016/j.lithos.2009.04.022

Dilek, Y. and Furnes, H. (2019): Tethyan ophiolite and Tethyan seaways. Journal of the Geological Society, 176, 899-912. https://doi.org/10.1144/jgs2019-129

Floyd, P. A. and Winchester, J. A. (1975): Magma type and tectonic setting discrimination using immobile elements. Earth and Planetary Science Letters, 27, 211-218. https://doi.org/10.1016/0012-821X(75)90031-X

Holt, A. F. and Condit, C. B. (2021): Slab Temperature Evolution Over the Lifetime of a Subduction Zone. Geochemistry, Geophysics, Geosystems, 22. https://doi.org/10.1029/2020GC009476

Irvine, T. N. and Baragar, W. R. A. (1971): A Guide to the Chemical Classification of the Common Volcanic Rocks. Canadian Journal of Earth Sciences, 8(5), 523-548. https://doi.org/10.1139/e71-055

Le Maitre, R. W., Bateman, P., Dudek, A., Keller, J., Lameyre, P., Le Bas, M.J., Sabine, P.A., Schmid, R., Sørensen, H., Streckeisen, A., Wooley, A.R. and Zanettin, B. (1989): A Classification of Igneous Rocks and Glossary of Terms. Recommendations of the IUGS Subcommision on the Systematics of Igneous Rocks. Blackwell; London, 204 p.

Kusky, T.M., Windley, B.F., Safonova, I., Wakita, K., Wakabayashi, J., Polat, A. and Santosh, M. (2013): Recognition of ocean plate stratigraphy in accretionary orogens through Earth history: a record of 3.8 billion years of sea floor spreading, subduction, and accretion. Gondwana Research, 24/2, 501-547. https://doi.org/10.1016/j.gr.2013.01.004

Majer, V. and Lugović, B. (1985): Metamorfne stijene u ofiolitnoj zoni Banije, Jugoslavija. II. Amfiboliti (metabaziti) (*Metamorphic rocks in the ophiolite zone in Banija, Yugoslavia, II. The amphibolites (metabasites)*). Acta geol., 15/2, 25-49. *(in Croatian – with English abstract)*

Miyashiro, A. (1975): Volcanic Rock Series and Tectonic Setting. Annual Review of Earth and Planetary Sciences, 3, 251-269. https://doi.org/10.1146/annurev.ea.03.050175.001343

Pearce, J. A. (1996): A users guide to basalt discrimination diagrams. In: Wyman, D. A. (ed.) Trace Element Geochemistry of Volcanic Rocks: Applications for Massive Sulphide Exploration. Geological Association of Canada, Short Course Notes 12, 79-113.

Robertson, A. H. F. (2002): Overview of the genesis and emplacement of Mesozoic ophiolites in the eastern Mediterranean Tethyan region. Lithos, 65, 1-67. https://doi.org/10.1016/S0024-4937(02)00160-3

Rollinson, H. R. (1993): Using geochemical data: evaluation, presentation, interpretation. Edinburgh Gate: Longman Scientific & Technical, 352 p.

Saccani, E. (2015): A new method of discriminating different types of post-Archean ophiolitic basalts and their tectonic significance using Th-Nb and Ce-Dy-Yb systematics. Geoscience Frontiers, 6 (4), 481-501. https://doi.org/10.1016/j.gsf.2014.03.006

Schmid, S. M., Bernoulli, D., Fügenschuh, B., Matenco, L., Schefer, S., Schuster, R., Tischler, M. and Ustaszewski, K. (2008): The Alpine–Carpathian–Dinaridic orogenic system: correlation and evolution of tectonic units. Swiss J. Geosci., 101, 139–183. https://doi.org/10.1007/s00015-008-1247-3

Schmid, M.S., Fügenschuh, B., Kounov, A., Matenco, L., Nievergelt, P., Oberhänsli, R., Pleuger, J., Schefer, S., Schuster, R., Tomljenović, B., Ustaszewski, K. and van Hinsbergen, D.J.J. (2020): Tectonic units of the Alpine collision zone between Eastern Alps and western Turkey. Gondwana Research, 78, 308-324. https://doi.org/10.1016/j.gr.2019.07.005

Shervais, J. W. (1982): Ti-V plots and the petrogenesis of modern and ophiolitic lavas. Earth and Planetary Science Letters 59, 101-118. https://doi.org/10.1016/0012-821X(82)90120-0

Slovenec, D. and Bermanec, V. (2003): Sistematska mineralogija – mineralogija silikata. *(Systematic mineralogy – mineralogy of silicates).* Denona, Zagreb, 359 p. *(in Croatian)*

Soret, M., Agard, P., Ildefonse, B., Dubacq, B., Prigent, C. and Rosenberg, C. (2019): Deformation mechanisms in mafic amphibolites and granulites: record from the Semail metamorphic sole during subduction infancy. Solid Earth, 10, 1733-1755. https://doi.org/10.5194/se-10-1733-2019

Sun, S. S. and McDonough, W. F. (1989): Chemical and isotopic systematics of oceanic basalts: implications for mantle composition and processes. Magmatism in the ocean basins. Geological Society, Special Publication, 42, 313-345. https://doi.org/10.1144/GSL.SP.1989.042.01.19

Šegvić, B., Slovenec, D., Altherr, R., Babajić, E., Mählmann, R.F. and Boško Lugović (2019): Petrogenesis of high-grade metamorphic soles from the central Dinaric ophiolite belt and their significance for the Neoththyan evolution in the Dinarides. Ofioliti, 44(1), 1-30.

Šegvić, B., Slovenec, D., Schuster, R., Babajić, E., Badurina, L. and Lugović, B. (2020): Sm-Nd geochronology and petrologic investigation of a sub-ophiolite metamorphic sole from the Dinarides (Krivaja-Konjuh Ophiolite Coplex, Bosnia and Herzegovina). Geologia croatica, 73/2, 119-130. https://doi.org/10.4154/gc.2020.09

Šikić, K. (2014): Osnovna geološka karta RH 1:100.000, Tumač za list Bosanski No-vi [Basic Geological Map of Republic Croatia 1:100.000, Geology of the Bosan-ski Novi sheet – In Croatian].– Croatian Geological Survey, Zagreb, 111 p.

Šikić, K., Buzaljko, R. and Mojićević, M. (1990): Tumač Osnovne geološke karte SFRJ 1:100.000 list Bosanski Novi. *(The interpreter of Basic Geological Map of the SFRJ, scale 1:100.00, sheet Bosanski Novi)*. Institut za geološka istraživanja, Zagreb, Savezni geološki zavod, Beograd. *(in Croatian – with English abstract)*

van Hinsbergen, D.J.J., Torsvik, T.H., Schmid, S.M., Matenco, L.C., Maffione, M., Vissers, R.L.M., Gürer, D. and Spakman, W. (2020): Orogenic architecture of the Mediterranean region and kinematic reconstruction of its tectonic evolution since the Triassic. Gondwana Research, 81, 9-229. https://doi.org/10.1016/j.gr.2019.07.009

Wada, I., Dehn, M.D. and Shaw, A.M. (2012): Effects of heterogeneous hydration in the incoming plate, slab rehydration, and mantle wedge hydration on slab-derived H_2O flux in subduction zones. Earth and Planetary Science Letters, 353-354, 60-71. https://doi.org/10.1016/j.epsl.2012.07.025

Wakabayashi, J. and Dilek, Y. (2003): What constitutes 'emplacement' of an ophiolite?: Mechanisms and relationship to subduction initiation and formation of metamorphic soles. Geological Society, London, Special Publications, 218, 427-447. https://doi.org/10.1144/GSL.SP.2003.218.01.22

Wilson, M. (1989): Igneous Petrogenesis. A Global Tectonic Approach. Chapman & Hall, London, 466 p.

Winchester, J. A. and Floyd, P. A. (1977): Geochemical discrimination of different magma series and their differentiation products using immobile elements. Chemical Geo-

Copyright held(s) by author(s), publishing rights belongs to publisher, pp. 97-110, DOI: 10.17794/rgn.2024.2.8

logy, 20, 325-343. https://doi.org/10.1016/0009-2541(77)90057-2

Wood, D. A. (1980): The application of a Th-Hf-Ta diagram to problems of tectonomagmatic classification and to establishing the nature of crustal contamination of basaltic lavas of the British Tertiary volcanic province. Earth and Planetary Science Letters, 50, 11-30. https://doi.org/10.1016/0012-821X(80)90116-8

SAŽETAK

Geokemija i petrografija amfibolita metamorfne podloge iz kamenoloma Slatina, Zrinska gora, Hrvatska

Istraživani amfiboliti Zrinske gore dio su metamorfne podloge ofiolitnoga kompleksa Banovine. Mineralni sastav i druge petrografske karakteristike istražene su polariziranom svjetlosnom mikroskopijom, a kemijske analize stijena dobivene su kombinacijom induktivno spregnute plazme s masenom i emisijskom spektrometrijom. Glavni minerali u ovim granatonosnim amfibolitima jesu amfibol i plagioklas s akcesornim granatom, sfenom, spinelom i opàkim mineralom te ± klinopiroksen ± kvarc, ± aktinolit, ± coisit-klinocoisit, ± prehnit, ± pumpelyit i ± glineni minerali. Amfiboliti imaju nematoblastične, nematogranoblastične, porfiroblastične i porfiroklastične strukture te homogene i trakaste teksture. Prisutnost klinopiroksena u nekim od istraživanih amfibolita sugerira njihovo moguće formiranje u P-T uvjetima gornjega amfibolitnog facijesa. Evidentni su također retrogradni metamorfizam u uvjetima facijesa zelenoga škriljavca kao i kasnije površinsko trošenje. Kemijski sastavi stijena upućuju na to da su protoliti većine amfibolita bili toleiitski bazalti, inicijalno formirani u području otočnih lukova i pripadajućih zalučnih bazena. Za vrijeme intraoceanske subdukcije u jurskome Neotetiskom oceanu bazalti / bazaltni tufovi s karakteristikama islandskih lučnih toleiita i bazalti pozadinskih lučnih bazena pozicionirani na vrhu oceanske ploče koja se podvlačila zavareni su u bazu vrućega iznadležećeg plaštnog klina, metamorfozirani u amfibolitne stijene i obducirani zajedno s ofiolitima na kontinentalni rub Jadranske ploče. Novoopisani tip amfibolita koji ima karakteristike peridotitnoga protolita nastao je kao posljedica hidratacije donjega dijela iznadležećega plaštnog klina.

Ključne riječi:
amfibolit, metamorfna podloga, peridotit, toleiitski bazalt, otočni luk, zalučni bazen

Author’s contribution

Principal author **Marija Putak Juriček (1)** (PhD, Research Associate at the Department of Mineralogy, Georg-August-Universität Göttingen, Petrology and Geochemistry) collected the samples in the field, conducted petrographic investigations, made the presentation of geochemical data in tables and diagrams, and wrote the manuscript.
Corresponding author **Vesnica Garašić (2)** (PhD, Associate Professor at the Faculty of Mining, Geology and Petroleum Engineering, University of Zagreb, Petrology and Geochemistry) initiated the investigation, provided funding for the field work and geochemical analyses, participated in the field work, gave suggestions in the interpretation of the research results and graphic presentation of data and participated in the writing of the discussion and conclusion sections.

Copyright held(s) by author(s), publishing rights belongs to publisher, pp. 97-110, DOI: 10.17794/rgn.2024.2.8